How to assess background activity: introducing a histogram-based analysis as a first step for accurate one-step PET quantification

Burger, Irene A ; Vargas, Hebert A ; Beattie, Brad J ; Goldman, Debra A ; Zheng, Junting ; Larson, Steven M ; Humm, John L ; Schmidtlein, Charles R

Abstract: Many common PET segmentation methods for malignant lesions use surrounding background activity as a reference. To date, background has to be measured by drawing a second volume of interest (VOI) in nearby, undiseased tissue. This is time consuming as two VOIs have to be determined for each lesion. The aim of our study was to analyse whether background activity in different organs and body regions could be calculated from the tumour VOI by histogram analyses. The institutional review board waived informed consent for this retrospective study. For each of the following tumour types and areas - head and neck (neck), lung, hepatic metastasis (liver), melanoma (skin), and cervix (pelvis) - 10 consecutive patients with biopsy-proven tumours who underwent (18)F-fluorodeoxyglucose-PET in January 2012 were retrospectively selected. One lesion was selected and two readers drew a cubical VOI around the lesion (VOItumour) and over the background (VOIBG). The mean value of VOIBG was compared with the mode of the histogram, using equivalence testing with an equivalence margin of ±0.5 SUV. Inter-reader agreement was analysed for the mean background, and the mode of the VOItumour histogram was assessed using the concordance correlation coefficient. For both readers, the mode of VOItumour was equivalent to the mean of VOIBG ($P<0.0001$ for R1 and R2). The inter-reader agreement was almost perfect, with a concordance correlation coefficient of greater than 0.92 for both the mode of VOItumour and the mean of VOIBG. Background activity determined within a tumour VOI using histogram analysis is equivalent to separately measured mean background values, with an almost perfect inter-reader agreement. This could facilitate PET quantification methods based on background values without increasing workload.

DOI: https://doi.org/10.1097/MNM.0000000000000045

Technical note

Nuclear Medicine Communications

How to assess background activity: introducing a histogram-based analysis as a first step for accurate one-step PET quantification

Irene A. Burger[a,d], Hebert A. Vargas[a], Brad J. Beattie[b], Debra A. Goldman[a], Junting Zheng[c], Steven M. Larson[a], John L. Humm[b] and Charles R. Schmidtlein[b]

Many common PET segmentation methods for malignant lesions use surrounding background activity as a reference. To date, background has to be measured by drawing a second volume of interest (VOI) in nearby, undiseased tissue. This is time consuming as two VOIs have to be determined for each lesion. The aim of our study was to analyse whether background activity in different organs and body regions could be calculated from the tumour VOI by histogram analyses. The institutional review board waived informed consent for this retrospective study. For each of the following tumour types and areas – head and neck (neck), lung, hepatic metastasis (liver), melanoma (skin), and cervix (pelvis) – 10 consecutive patients with biopsy-proven tumours who underwent ^{18}F-fluorodeoxyglucose-PET in January 2012 were retrospectively selected. One lesion was selected and two readers drew a cubical VOI around the lesion (VOI_{tumour}) and over the background (VOI_{BG}). The mean value of VOI_{BG} was compared with the mode of the histogram, using equivalence testing with an equivalence margin of ±0.5 SUV. Inter-reader agreement was analysed for the mean background, and the mode of the VOI_{tumour} histogram was assessed using the concordance correlation coefficient. For both readers, the mode of VOI_{tumour} was equivalent to the mean of VOI_{BG} ($P < 0.0001$ for R1 and R2). The inter-reader agreement was almost perfect, with a concordance correlation coefficient of greater than 0.92 for both the mode of VOI_{tumour} and the mean of VOI_{BG}. Background activity determined within a tumour VOI using histogram analysis is equivalent to separately measured mean background values, with an almost perfect inter-reader agreement. This could facilitate PET quantification methods based on background values without increasing workload. *Nucl Med Commun* 35:316–324 © 2014 Wolters Kluwer Health | Lippincott Williams & Wilkins.

Nuclear Medicine Communications 2014, **35**:316–324

Keywords: background definition, ^{18}F-fluorodeoxyglucose quantification, histogram mode, PET segmentation, semiautomatic

Departments of [a]Radiology, [b]Medical Physics, [c]Epidemiology-Biostatistics, Memorial Sloan-Kettering Cancer Center, New York, New York, USA and [d]Department of Radiology, University Hospital Zurich, Zurich, Switzerland

Correspondence to Irene A. Burger, MD, Department of Radiology, University Hospital Zurich, Ramistrasse 100, 8091 Zurich, Switzerland
Tel: +41 44 255 11 11; fax, +41 44 255 44 14;
e-mail: irene.burger@usz.ch

Received 26 July 2013 **Revised** 3 October 2013 **Accepted** 21 October 2013

Introduction

The ability of ^{18}F-fluorodeoxyglucose (^{18}F-FDG) PET/computed tomography (CT) to provide a quantitative estimation of tumour burden has played an important role in its success in therapy response assessment [1]. Currently, the most commonly used quantification method in routine clinical practice is the maximum standardized uptake value (SUV_{max}), normalized either to weight, lean body mass or body surface [2]. Although there are several advantages in the use of SUV_{max}, including ease of measurement and good interobserver reproducibility, there are also major limitations, such as the high statistical noise that derives from a single voxel analysis [3–5]. In addition, SUV measurements do not take into account the amount of physiologic background (BG) activity, which varies between different anatomical sites and different patients, thus making it impossible to use absolute SUV cutoff values to separate normal physiological activity from malignant or inflammatory activity.

To estimate the PET volume, an SUV_{max}-based threshold method (42% of the SUV_{max}) was introduced [6]. Because of the heterogeneous nature of tumours and the surrounding tissues, however, this method was found to be inaccurate in several studies [7–9]. Multiple methods have been proposed to deal with the limitation of ^{18}F-FDG PET volume determination. Central to most of these approaches is defining the average BG activity around the lesion on PET images. Nestle *et al.* [9] proposed a BG-based correction, subtracting the mean BG and 15% from the peak activity (70% of the hottest voxels) for spill-over correction, and found that this approach significantly improved the accuracy of measured tumour volumes in PET scans. Daisne *et al.* [10] suggested an automated lesion-to-BG ratio-adapted threshold to integrate BG activity into tumour segmentation methods, which has been shown to yield a higher accuracy compared with multiple simple threshold-based volume segmentation tools [11,12].

0143-3636 © 2014 Wolters Kluwer Health | Lippincott Williams & Wilkins DOI: 10.1097/MNM.0000000000000045

Although the need to account for BG activity when quantifying tracer uptake is generally accepted [1], there is no agreement on how this should be measured. Some authors propose using a volume of interest (VOI) placed over the region adjacent to the tumour with the highest activity [9,13], whereas others prefer the use of a population-based BG value for different areas (e.g. soft tissue and bone) [14]. Both of these approaches are acceptable; however, the former is time consuming and observer dependent, particularly in a clinical setting with multiple lesions per patient, whereas the latter may not be applicable to organs that are known to have wide variability in BG activity among different patients, such as the liver. Drever and colleagues [15,16] used a histogram-based analysis to determine BG activity in phantom studies to determine a local contrast-based approach for threshold segmentation of PET volumes. If this principle was robust enough to yield reliable values for BG activity in the much more heterogeneous and tumour and BG setting of real patients, this could be a valuable alternative to manually drawn adjacent VOIs or population-based BG values. To our knowledge this has never been followed up with patient data.

Thus, the purpose of this study was to automatically derive the BG activity from the tumour VOI, using simple histogram analysis, and to test the robustness of the method for different reconstruction algorithms in phantoms and within different organs with variable tumour-to-BG ratios in patients.

Materials and methods

Phantom analysis

To test for the robustness of the histogram-based BG measurement under different image reconstruction methods affecting image resolution or noise, we selected a phantom with a homogeneous BG: a standard American College of Radiology (ACR; flangeless Esser PET Phantom; Data Spectrum Corporation, Durham, North Carolina, USA) cylindrical phantom with separately fillable cylinders, used for scanner quality assurance testing (Fig. 1a). The scan was performed in accordance with the ACR guidelines, assuming a 70 kg patient with a 444 MBq injection as the reference (36 MBq for the BG and 16 MBq diluted in 1000 cm^3 for the hot cylinder volumes). After filling the BG volume (6.3 l), the phantom had a homogeneous BG with a mean SUV of 1. After 60 min, the phantom was scanned for 3 min. The data were reconstructed at 10, 15, 20, 30, 45, 60, 90 and 180 s, resulting in a continuous decrease in noise and increase in contrast resolution. In addition the 3-min scan was reconstructed using one, two, three or four iterations each using 20 subsets and two different matrix sizes of 128 and 256 with 6.3 mm postreconstruction smoothing and three-point [121] z-axis smoothing. A VOI_{lesion} was placed over the largest cylinder. The mode of the histogram was defined as the most common voxel value in the VOI_{lesion} and was compared with the mean VOI_{BG} (Fig. 2).

To assess the influence of an increase in VOI size on the mode of the histogram, a phantom with a heterogeneous BG was selected. The Society of Nuclear Medicine Clinical Trials Network (SNM-CTN) anthropomorphic thorax phantom (Chest Oncology Phantom) was filled in accordance with the SNM-CTN instructions and reconstructed using our clinical settings: ordered subset expectation maximization (OSEM) with two iterations over 20 subsets, 6.3-mm postreconstruction transaxial filtering and three-point [121] smoothing along the z-axis (Fig. 1b). A cubical VOI was placed around a spherical lesion, abutting the edges of the lesion with an edge length of 30 mm. Thereafter, the diameter of the VOI_{lesion} was continuously enlarged over four steps, yielding five $VOI_{lesions}$ with an increasing size. The mode of each histogram for the $VOI_{lesions}$ was determined. As a reference, the mean SUV in a fixed-size cubical VOI_{BG} was used (Fig. 3).

Patient selection

The Institutional Review Board waived the informed consent requirement for this retrospective study. Patients who underwent ^{18}F-FDG PET/CT at our institution for routine clinical purposes between January 2012 and March 2012 were screened. To address a large variety of tumour-to-BG ratios, we included 50 patients, 10 consecutive patients with known malignancies in five different areas: head and neck squamous cell carcinoma (neck), non-small-cell lung cancer (lung), hepatic metastasis of colon cancer (liver), cutaneous melanoma (skin) and uterine cervical cancer (pelvis).

Image acquisition

All patients underwent PET/CT on a Discovery STE or Discovery 600/690 system (GE Medical Systems, Waukesha, Wisconsin, USA); 60 min after the injection of 400–500 MBq (nominally 444 MBq) of ^{18}F-FDG, a low-dose attenuation-correction CT scan (120–140 kV, ~80 mA with patient-specific variations) was acquired. This was followed by acquisition of PET emission images from the pelvis to the skull. Attenuation correction was routinely applied and images were reconstructed using iterative algorithms (GE DSTE – OSEM with two iterations over 20 subsets and 6.3 mm postreconstruction axial filtering and three-point [121] smoothing along the z-axis and GE D690 ToF/PSF OSEM with two iterations over 16 subsets and 6.0 mm postreconstruction transaxial filtering and three-point [121] smoothing along the z-axis). Before the examination, patients were asked to fast for at least 6 h, but liberal intake of water was allowed.

Image analysis

One lesion per patient was identified for analysis. Two readers (R1/R2) independently placed cubical VOIs around each lesion (VOI_{tumour}). First, a large VOI_{tumour}

Fig. 1

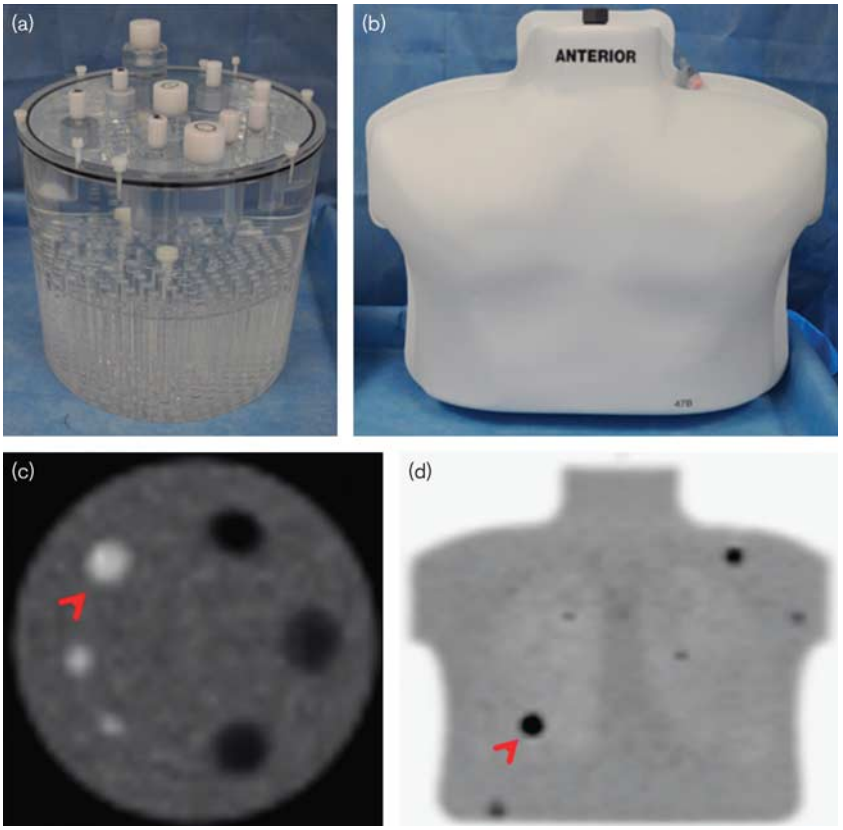

(a) To test the robustness of the histogram-based background calculation under different image reconstruction settings, a standard American College of Radiology (ACR) cylindrical phantom (flangeless Esser PET Phantom) was used. (b) To assess the influence of the volume of interest (VOI) size on the background estimation, a Society of Nuclear Medicine Clinical Trials Network (SNM-CTN) anthropomorphic thorax phantom was used. (c) Axial image of the cylindrical phantom, which was filled and scanned according the ACR guidelines. (d) Coronal maximum-intensity projection image of the thorax phantom, which was filled in accordance with the SNM-CTN instructions and reconstructed using our clinical settings. One lesion was selected in both phantoms for further analysis (red arrow).

Fig. 2

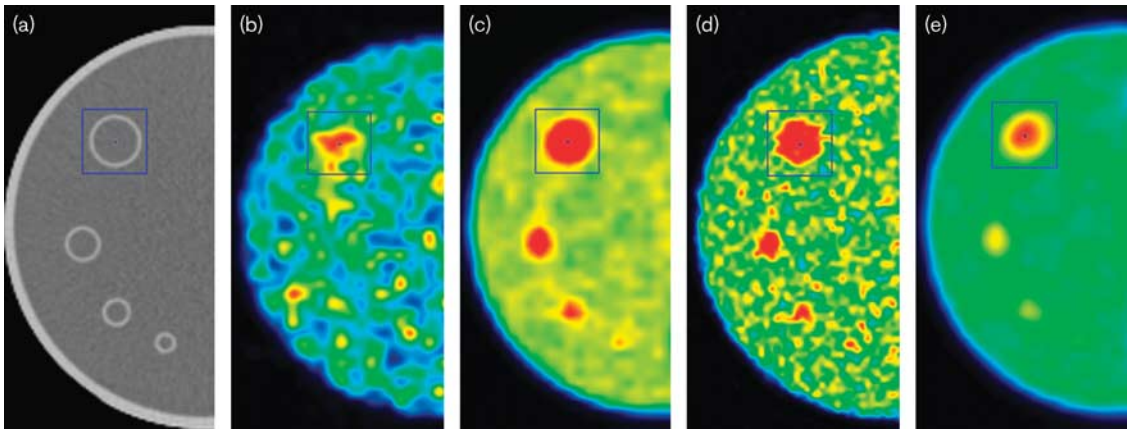

(a) Axial CT image of the ACR cylindrical phantom with the VOI around the selected cylinder. (b–e) Four examples of axial ^{18}F-FDG PET images of the same slice after different image reconstructions: (b) with a 10-s acquisition time, (c) with a 3-min acquisition time, (d) with four iterations and 20 subsets each with a matrix size of 128 and (e) with only one iteration and 20 subsets and a matrix of 256. ACR, American College of Radiology; CT, computed tomography; ^{18}F-FDG, ^{18}F-fluorodeoxyglucose; VOI, volume of interest.

Fig. 3

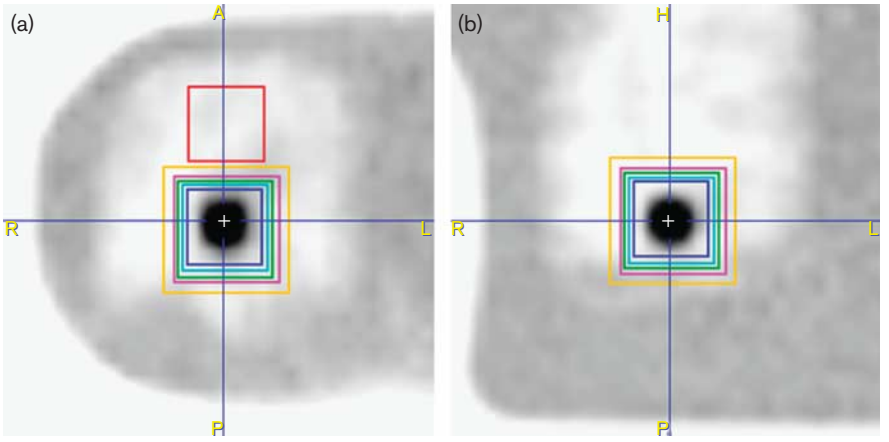

^{18}F-fluorodeoxyglucose (a) axial and (b) coronal PET images of the anthropomorphic thorax phantom with simulated lung lesions, illustrating the different volume of interest (VOI) sizes placed around the selected lesions, with a 30 mm (dark blue) to 50 mm (orange) edge length. A background VOI (VOI_{BG}, red) was placed adjacent, with an edge length of 30 mm. The mean standardized uptake value (SUV) in the VOI_{BG} is 0.49 SUV. The mode of the VOI_{lesion}, defined as the most common voxel value in the VOI_{lesion}, ranged from 0.50–0.54 SUV.

Fig. 4

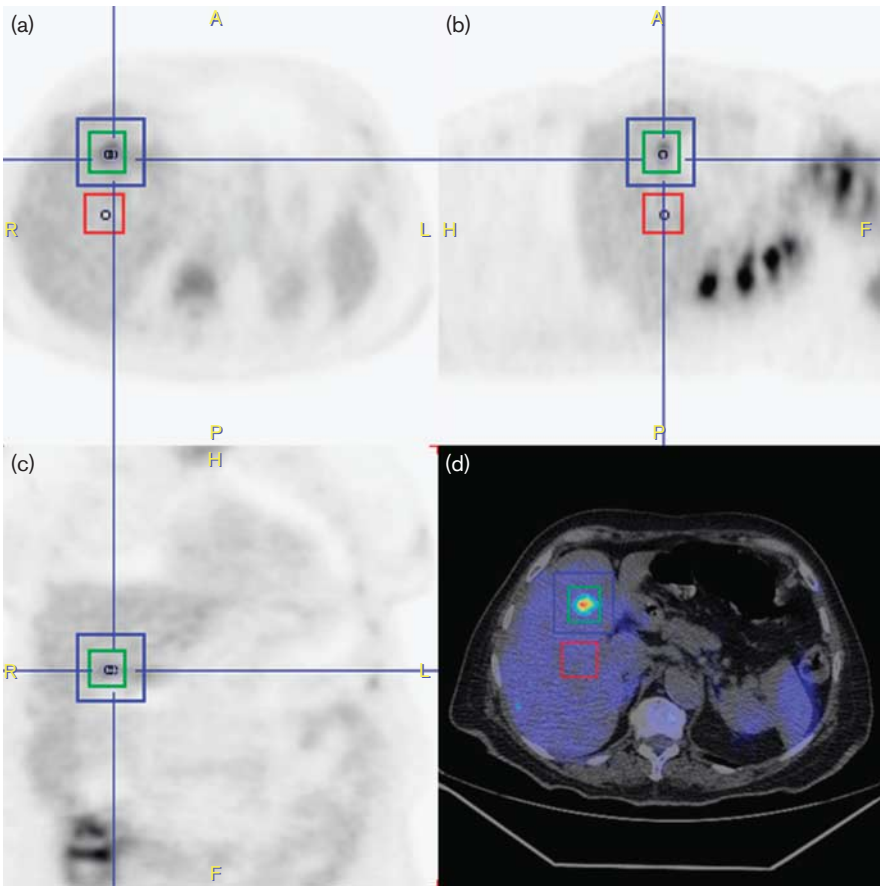

^{18}F-FDG PET images of hepatic metastasis of colon cancer (patient 7) with the inserted volumes of interests (VOIs) by reader 1 in (a) axial, (b) sagittal and (c) coronal planes. (d) An additional axial fused ^{18}F-FDG PET/CT image with three VOIs: a large VOI (VOI_L; blue), a small VOI (VOI_S; green, which is just abutting the tumour margins) and the separate VOI_{BG} (red) over healthy tissue. CT, computed tomography; BG, background; ^{18}F-FDG, ^{18}F-fluorodeoxyglucose.

Fig. 5

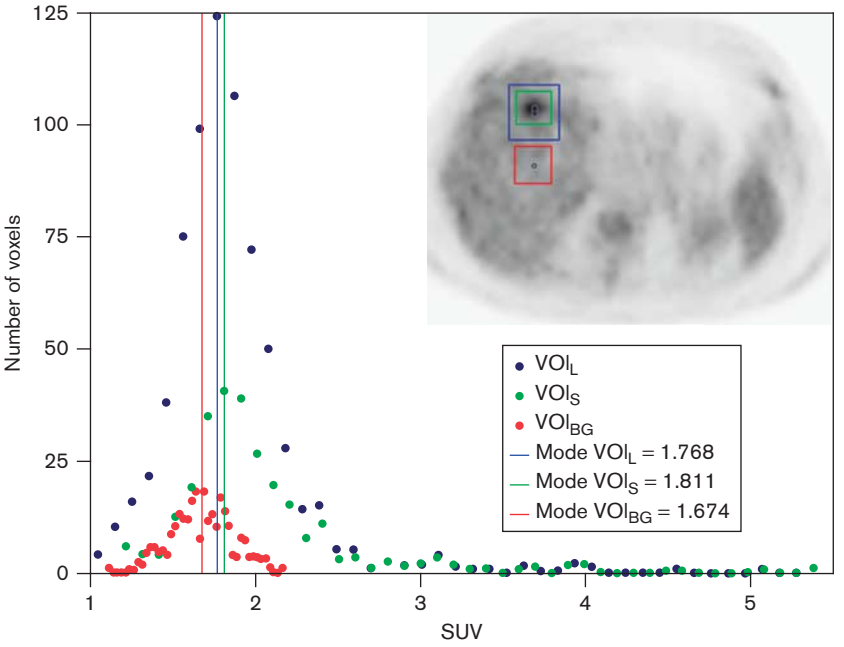

The three rebinned and scaled histograms derived from the large (blue) and the small (green) tumour volumes of interest (VOI_{tumour}), as well as the background VOI (VOI_{BG}; red) of the same lesion as in Fig. 1, with the VOIs illustrated on a transverse ^{18}F-FDG PET plane in the right upper corner. The mean background value (1.676 SUV) is nearly identical to the mode of the histogram in VOI_{BG} (1.674 SUV) and is very close to the mode of the histogram values in both the large (1.768 SUV) and the small (1.811 SUV) VOI_{tumour}. ^{18}F-FDG, ^{18}F-fluorodeoxyglucose; VOI, volume of interest; SUV, standardized uptake value.

Table 1 Phantom study results

ACR phantom – acquisition time (s)	Mode VOI_{lesion} (SUV)	Mean VOI_{BG} (SUV)
10	0.81	0.93
15	0.86	0.95
20	0.99	0.93
30	0.96	1.04
45	0.99	1.02
60	0.98	1.02
90	0.95	1.02
180	1.03	1.01
ACR phantom – reconstruction: iteration × subsets (matrix)	Mode VOI_{lesion} (SUV)	Mean VOI_{BG} (SUV)
1 × 20 (128)	1.03	1.01
2 × 20 (128)	1.10	1.01
3 × 20 (128)	1.07	1.01
4 × 20 (128)	1.06	1.01
1 × 20 (256)	1.06	1.01
2 × 20 (256)	1.01	1.01
3 × 20 (256)	1.01	1.01
4 × 20 (256)	0.99	1.02
Thorax phantom – increasing VOI edge length (mm)	Mode VOI_{lesion} (SUV)	Mean VOI_{BG} (SUV)
30	0.51	0.49
34	0.54	0.49
38	0.50	0.49
42	0.50	0.49
50	0.50	0.49

ACR, American College of Radiology; SUV, standard uptake value; VOI_{BG}, background volume of interest; VOI_{lesion}, lesion volume of interest.

(VOI_L) was drawn generously around the lesion with the margins of the VOI placed more than 1 cm away from the edge of the lesion. Thereafter, a small VOI_{tumour} (VOI_S) was drawn tightly around the lesion with the margin of the VOI abutting the edge of the lesion. For each patient, a third VOI was placed in a region away from the lesion but within the same organ to determine the mean BG (VOI_{BG}) (Fig. 4). For each VOI, care was taken not to include increased ^{18}F-FDG activity from adjacent structures (e.g. excreted tracer in the bladder/ureter).

Table 2 **Difference between the mean VOI_{BG} and the mode of the histograms of VOI_L and VOI_S**

	Reader 1		Reader 2	
	MH VOI_L – mean VOI_{BG}	MH VOI_S – mean VOI_{BG}	MH VOI_L – mean VOI_{BG}	MH VOI_S – mean VOI_B
Mean	0.0007	0.1778	–0.0011	0.1877
SD	0.3025	0.4231	0.334	0.3982
Range	–1.0022 to 0.8438	–0.9913 to 1.3254	–0.7341 to 1.1881	–0.7053 to 1.5014
Two-sided 95% CI of the mean	–0.0831 to 0.0846	–0.0605 to 0.2951	–0.0937 to 0.0915	–0.0774 to 0.2981
Equivalence conclusion	Yes	Yes	Yes	Yes

CI, confidence interval; MH, mode of the histogram; VOI_{BG}, background volume of interest; VOI_L, large volume of interest; VOI_S, small volume of interest.

Fig. 6

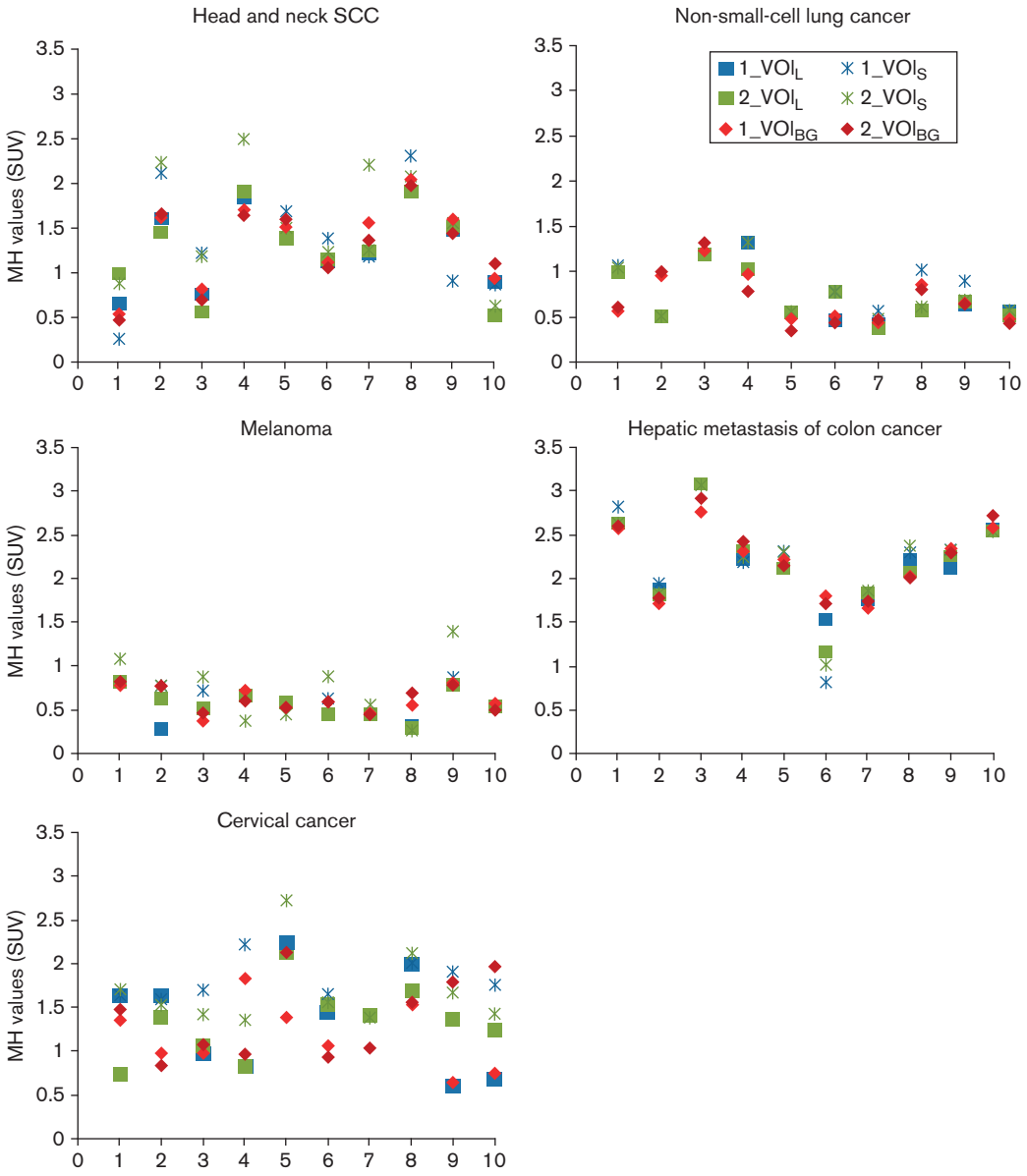

Overview of all patients (1–10) for each tumour type: the mode of the histogram (MH), defined as the most common voxel value within a volume of interest (VOI), given for both readers (reader 1, blue; reader 2, green) and both the large VOI (VOI_L, square) and the small VOI (VOI_S, star) compared with the mean VOI_{BG} (diamonds, red). The most significant equivalence is reached in areas with homogeneous BG (lung, skin or liver). For lesions in the small pelvis (cervical cancer) the variability is higher, but this is also true for separately drawn dedicated VOI_{BG}. BG, background; SCC, squamous cell carcinoma; SUV, standardized uptake value.

In accordance with that in the study by Nestle *et al.* [9] for lesions surrounded by tissues with different ^{18}F-FDG activities (e.g. lung and liver/soft tissue and air), the structure with a visually higher ^{18}F-FDG uptake was defined as a 'relevant BG'.

The geometrical basis of VOI analysis with a most commonly round lesion captured within a square VOI leads to a ratio of BG-to-tumour voxels of nearly 1 or more. Therefore, the more homogeneous BG is represented by the mode of the histogram. The mode values for the histograms VOI_S and VOI_L were compared with the mean VOI_{BG} value.

Histograms representing the number of voxels (*x*-axis) for every SUV (*y*-axis) within a selected VOI were built for VOI_{lesion}, as well as VOI_L and VOI_s of both readers, for the phantom studies and exported using dedicated software (Pmod 3.3; Pmod Technologies, Zurich, Switzerland). The software automatically subdivided the SUVs within the VOI into 256 equal-sized bins. First, all voxels with an SUV below 0.1 were truncated from the histograms to remove the extra corporeal parts of the VOI. To calculate the mode of the histogram the values were rebinned by an empirical factor of 1/6 to find an acceptable tradeoff between resolution and noise in the BG area. The mode was determined from the resulting histogram (Fig. 5).

Statistical analysis

An equivalence test with an equivalence margin of 0.5 SUV was used to compare the mean value of VOI_{BG} with the mode of the histogram of VOI_S and VOI_L for each reader separately. Concordance correlation coefficient (CCC) was used to assess interobserver agreement between mode of the histogram of VOI_S and VOI_L and the mean values of VOI_{BG} for readers one and two (R1, R2). Statistical analyses were carried out on SAS 9.2 (SAS Institute Inc., Cary, North Carolina, USA).

Results

Phantom data

The expected BG value of an SUV_{mean} of 1 for the ACR phantom was found to be highly reproducible, regardless of image noise, chosen reconstruction parameters or matrix size (Table 1). In addition, the gradual increase in the size of VOI_{lesion} from 30 to 50 mm edge length did not change the mode of the histogram (SUV 0.5–0.54) in the thorax phantom study, which was nearly identical to the mean of the VOI_{BG} (SUV_{mean} 0.49) (Table 1).

Table 3 Concordance correlation coefficient

	CCC	95% CI
MH VOI_L	0.943	0.912, 0.974
MH VOI_S	0.932	0.895, 0.969
Mean VOI_{BG}	0.920	0.877, 0.963

CCC, concordance correlation coefficient; CI, confidence interval; MH, mode of the histogram; VOI_{BG}, background volume of interest; VOI_L, large volume of interest; VOI_S, small volume of interest.

Patient data

For both readers, the mode of the histogram of both VOI_L and VOI_S was equivalent to the mean BG over all tumour groups (Table 2, Fig. 6).

The inter-reader agreement was very high, with a CCC of 0.920 (95% confidence interval: 0.877–0.963) for the mean BG, and 0.943 and 0.932, respectively, for the mode of the histogram of VOI_L and VOI_S (Table 3).

Discussion

Our study demonstrates that the mean BG activity can be accurately estimated using a single cubical VOI placed around a tumour. It also confirms the applicability of the geometrical principle stating that for a round or roundish tumour captured within a square VOI_{tumour} of the same size, the ratio of BG-to-tumour voxels is nearly 1 : 1 (Fig. 7). Therefore, the more homogeneous BG was well represented by the mode of the histogram of the VOI_{tumour} for all tumour types and both VOI sizes.

Histogram analysis for BG definition has been proposed in phantom studies by assuming that the second peak in the histogram corresponds to the mean BG activity, as a large portion of the VOI contained air [15,16]. However, to our knowledge, this has never been investigated using real patient data.

Commonly, BG activity for ^{18}F-FDG quantification is determined by placing a dedicated VOI_{BG} away from the tumour in adjacent tissue. It has been observed that BG values are stable within different VOI_{BG}, as ^{18}F-FDG activity is rather homogeneous within normal organs [9]. However, our results show that the inter-reader variability of VOI_{BG} values is comparable with that in the analysis of BG activity with the mode of the histogram. An atlas-based method to correct for BG activity was proposed for the quantitative assessment of prostate cancer metastasis by measuring SUV_{max} in the iliac crest and gluteal muscle in 65 scans, subtracting the mean SUV_{max} of bone in osseous lesions and the mean SUV_{max} value of the gluteal muscle for lymph node metastasis [14]. This is reasonable in tissue with small variability in ^{18}F-FDG activity among different patients; however, for lesions in the liver or pelvis, it does not seem to be feasible.

Clinical guidelines gaining more and more acceptance suggest the use of BG-based methods for PET volume measurement [1]. This has been implemented for BG-activity-based methods using a dedicated VOI_{BG} for each lesion to determine PET volume and has been shown to be more accurate than a threshold-based analysis [11]. With the presented method, BG values could now be automatically integrated into clinical lesion analysis.

Fig. 7

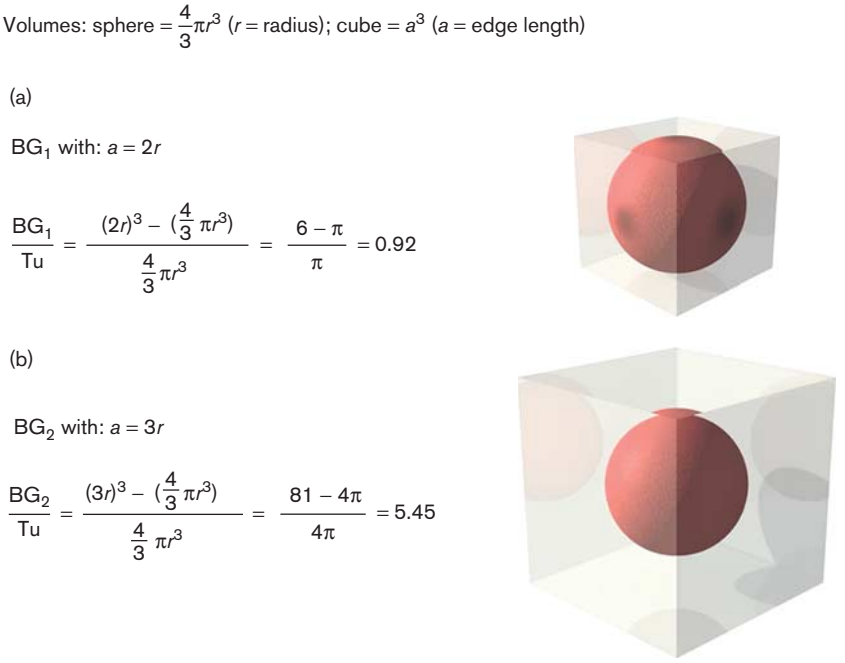

Illustration of the mathematical relation of the background (BG)-to-tumour volume ratio for an ideal cubical volume of interest (VOI) around a spherical lesion: (a) for a cubical VOI with the same size as the lesion diameter, the BG-to-tumour ratio is nearly 1. (b) With only a slight increase in the VOI size, such as a cube length three times the radius, more than 80% of the voxels within the VOI represent BG and less than 20% are within the lesion. Tu, tumour.

The technique is highly reproducible, as shown by the high degree of agreement among patients, with a CCC of greater than 0.9 for all measurements between two independent readers, as well as by the phantom data that gave stable results for a wide variety of reconstruction methods, signal-to-noise ratios and VOI sizes. When drawing a VOI_{tumour} for BG analysis in a patient, especially if the tumour is surrounded by two different tissues, one consideration has to be followed: the most active part must be regarded as the relevant BG and needs to be dominant in the VOI_{tumour}. Therefore, more voxels of the VOI have to be in the area with higher BG activity. This simple consideration could be followed by both observers and might have contributed to the high CCC, even in more challenging areas such as the liver dome (liver/lung interface) or cutaneous lesions (soft tissue/air interface).

In clinical routine, a dedicated VOI_{BG} would likely increase the workload and would also have to be integrated into the clinical workstation to link the VOI_{BG} with the corresponding VOI_{tumour} for each lesion. This is especially important for patients with extensive disease and would likely increase the evaluation time and effort. One of the strengths of our proposed histogram-based BG analysis is that it can be integrated with modest programming effort as an automated feature in existing vendor software, facilitating more quantitative PET analysis and tumour segmentation without increasing clinical work.

The present study is only the first step in a potential histogram-based PET quantification. It was carried out to show that the BG can be determined irrespective of the organ site or reconstruction algorithm. Further limitations were the small sample sizes per tumour entity. However, our goal was to find a method to reliably measure BG activity throughout the body. Therefore, an analysis of a variety of different organ systems with validation of the overall equivalence was chosen. In addition, when binning the derived data for histogram analysis we chose an empirical factor based on visual interhistogram comparison to achieve an acceptable tradeoff between resolution and noise in the BG area. We are aware that other methods exist for doing this and that the factor used will depend on the presetting, which varies for different software solutions [17–19]. Finally, the method that we used to analyse BG activity requires a dedicated software that, although relatively simple, is not currently available in standard clinical viewing software packages. Modification of the existing vendor software would be necessary to facilitate this approach for more quantitative PET analysis.

Conclusion

A simple histogram analysis of the tumour VOI can enable automatic and accurate determination of the mean BG activity on PET images. This could lead to a more accurate PET quantification method to assess the total tumour activity, without any increase in workload.

Acknowledgements

The authors thank Pmod Technologies (Switzerland) for providing us with the software. Irene A. Burger was financially supported by the Dr Max Cloëtta Foundation (Switzerland) and the Swiss Society of Nuclear Medicine.

Conflicts of interest

There are no conflicts of interest.

References

1 Wahl RL, Jacene H, Kasamon Y, Lodge MA. From RECIST to PERCIST: evolving considerations for PET response criteria in solid tumors. *J Nucl Med* 2009; **50 (Suppl 1)**:122S–150S.
2 Boellaard R, O'Doherty MJ, Weber WA, Mottaghy FM, Lonsdale MN, Stroobants SG, *et al.* FDG PET and PET/CT: EANM procedure guidelines for tumour PET imaging: version 1.0. *Eur J Nucl Med Mol Imaging* 2010; **37**:181–200.
3 Burger IA, Huser DM, von Schulthess GK, Trinckauf J, Burger C, Buck A. Repeatability of FDG quantification in tumor imaging: averaged SUVs are superior to SUVmax. *Nucl Med Biol* 2012; **39**:666–670.
4 Schwartz J, Humm JL, Gonen M, Kalaigian H, Schoder H, Larson SM, *et al.* Repeatability of SUV measurements in serial PET. *Med Phys* 2011; **38**:2629–2638.
5 De Langen AJ, Vincent A, Velasquez LM, van Tinteren H, Boellaard R, Shankar LK, *et al.* Repeatability of ^{18}F-FDG uptake measurements in tumors: a metaanalysis. *J Nucl Med* 2012; **53**:701–708.
6 Erdi YE, Mawlawi O, Larson SM, Imbriaco M, Yeung H, Finn R, *et al.* Segmentation of lung lesion volume by adaptive positron emission tomography image thresholding. *Cancer* 1997; **80**:2505–2509.
7 Biehl KJ, Kong FM, Dehdashti F, Jin JY, Mutic S, El Naqa I, *et al.* ^{18}F-FDG PET definition of gross tumor volume for radiotherapy of non-small cell lung cancer: is a single standardized uptake value threshold approach appropriate? *J Nucl Med* 2006; **47**:1808–1812.
8 Hatt M, Cheze le Rest C, Turzo A, Roux C, Visvikis D. A fuzzy locally adaptive Bayesian segmentation approach for volume determination in PET. *IEEE Trans Med Imaging* 2009; **28**:881–893.
9 Nestle U, Kremp S, Schaefer-Schuler A, Sebastian-Welsch C, Hellwig D, Rube C, *et al.* Comparison of different methods for delineation of ^{18}F-FDG PET-positive tissue for target volume definition in radiotherapy of patients with non-small cell lung cancer. *J Nucl Med* 2005; **46**:1342–1348.
10 Daisne JF, Sibomana M, Bol A, Doumont T, Lonneux M, Gregoire V. Tri-dimensional automatic segmentation of PET volumes based on measured source-to-background ratios: influence of reconstruction algorithms. *Radiother Oncol* 2003; **69**:247–250.
11 Tylski P, Stute S, Grotus N, Doyeux K, Hapdey S, Gardin I, *et al.* Comparative assessment of methods for estimating tumor volume and standardized uptake value in (18)F-FDG PET. *J Nucl Med* 2010; **51**:268–276.
12 Francis RJ, Byrne MJ, van der Schaaf AA, Boucek JA, Nowak AK, Phillips M, *et al.* Early prediction of response to chemotherapy and survival in malignant pleural mesothelioma using a novel semiautomated 3-dimensional volume-based analysis of serial ^{18}F-FDG PET scans. *J Nucl Med* 2007; **48**:1449–1458.
13 Schaefer A, Kremp S, Hellwig D, Rube C, Kirsch CM, Nestle U. A contrast-oriented algorithm for FDG-PET-based delineation of tumour volumes for the radiotherapy of lung cancer: derivation from phantom measurements and validation in patient data. *Eur J Nucl Med Mol Imaging* 2008; **35**:1989–1999.
14 Fox JJ, Autran-Blanc E, Morris MJ, Gavane S, Nehmeh S, Van Nuffel A, *et al.* Practical approach for comparative analysis of multilesion molecular imaging using a semiautomated program for PET/CT. *J Nucl Med* 2011; **52**:1727–1732.
15 Drever L, Roa W, McEwan A, Robinson D. Iterative threshold segmentation for PET target volume delineation. *Med Phys* 2007; **34**:1253–1265.
16 Drever L, Robinson DM, McEwan A, Roa W. A local contrast based approach to threshold segmentation for PET target volume delineation. *Med Phys* 2006; **33**:1583–1594.
17 Scott DW. On optimal and data-based histograms. *Biometrika* 1979; **66**:605–610.
18 Freedman D, Diaconis P. On the histogram as a density estimator – L2 theory. *Z Wahrscheinlichkeit* 1981; **57**:453–476.
19 Shimazaki H, Shinomoto S. A method for selecting the bin size of a time histogram. *Neural Comput* 2007; **19**:1503–1527.